Phase Noise in Oscillators: DAEs and Colored Noise Sources

Alper Demir

alpdemir @research.bell-labs.com

Bell Laboratories
Murray Hill, New Jersey, USA

Abstract

Oscillators are key components of electronic systems. Undesired perturbations, i.e. noise, in practical electronic systems adversely affect the spectral and timing properties of oscillators resulting in *phase noise*, which is a key performance limiting factor, being a major contributor to bit-error-rate (BER) of RF communication systems, and creating synchronization problems in clocked and sampled-data systems. In this paper, we first present a theory and numerical methods for nonlinear perturbation and noise analysis of oscillators described by a system of *differential-algebraic equations* (DAEs), which extends our recent results on perturbation analysis of autonomous ordinary differential equations (ODEs). In developing the above theory, we rely on novel results we establish for linear periodically time-varying (LPTV) systems: Floquet theory for DAEs. We then use this nonlinear perturbation analysis to derive the stochastic characterization, including the resulting oscillator spectrum, of phase noise in oscillators due to *colored* (e.g., $1/f$ noise), as opposed to white, noise sources. The case of white noise sources has already been treated by us in a recent publication. The results of the theory developed in this work enabled us to implement a rigorous and effective analysis and design tool in a circuit simulator for low phase noise oscillator design.

1 Introduction

Oscillators are ubiquitous in physical systems, especially electronic and optical ones. For example, in radio frequency (RF) communication systems, they are used for frequency translation of information signals and for channel selection. Oscillators are also present in digital electronic systems which require a time reference, i.e., a clock signal, in order to synchronize operations.

Noise is of major concern in oscillators, because introducing even small noise into an oscillator leads to dramatic changes in its frequency spectrum and timing properties. This phenomenon, peculiar to oscillators, is known as *phase noise* or *timing jitter*. A perfect oscillator would have localized tones at discrete frequencies (i.e., harmonics), but any corrupting noise spreads these perfect tones, resulting in high power levels at neighboring frequencies. This effect is the major contributor to undesired phenomena such as interchannel interference, leading to increased bit-error-rates (BER) in RF communication systems. Another manifestation of the same phenomenon, timing jitter, is important in clocked and sampled-data systems: uncertainties in switching instants caused by noise lead to synchronization problems. Characterizing how noise affects oscillators is therefore crucial for practical applications. The problem is challenging, since oscillators constitute a special class among noisy physical systems: their *autonomous* nature makes them unique in their response to perturbations.

In a recent publication [1] (which has a brief review of previous work on phase noise), we presented a theory and numerical methods for practical characterization of phase noise in oscillators described by a system of *ordinary differential equations* (ODEs) with *white* noise sources. In this paper, we extend our results to oscillators described by a system of *differential-algebraic equations* (DAEs) with *colored* as well as white noise sources. The extension to DAEs and colored noise sources is crucial for implementing an effective analysis and design tool for phase noise in a a circuit simulator. Almost all of the circuit simulators use the MNA (Modified Nodal Analysis) formulation, which is basically a system of DAEs. Colored noise sources such as $1/f$ noise has a significant impact on phase noise of practical oscillators. Understanding how colored noise sources affect the oscillator spectrum is crucial for low phase noise, low cost, integrated oscillator designs that can meet the stringent specifications of today's RF communications applications.

First, in Section 2, we establish the equivalent of Floquet theory (and some related results) for periodically time-varying systems of linear DAEs, which we then use in Section 3 to develop the theory and numerical methods for nonlinear perturbation analysis of autonomous DAEs. In Section 4, we analyze the case of colored noise perturbations and obtain a stochastic characterization of the phase deviation. Models for burst (popcorn) and $1/f$ (flicker) noise, the most significant colored noise sources in IC devices, are discussed in Section 5. Then, in Section 6, we calculate the resulting oscillator spectrum with phase noise due to a colored noise source. Our treatment of phase noise due to colored noise sources is general, i.e., it is not specific to a particular type of colored noise source. Hence, our results are applicable to the characterization of phase noise due to not only $1/f$ and burst noise, but also other types of possibly colored noise, e.g., substrate or power supply noise. In Section 7, we consider the presence of white and colored noise sources together, and derive the resulting oscillator spectrum. Finally, in Section 8, we present simulation results in phase noise characterization of oscillators. All proofs are omitted due to space limitations.

2 Floquet theory for DAEs

We now consider the n-dimensional inhomogeneous linear system of DAEs[1]

$$\frac{d}{dt}\left(C(t)x\right)+G(t)x+b(t)=0 \tag{1}$$

where the matrix $C(\cdot):\mathbb{R}\rightarrow\mathbb{R}^{n\times n}$ is not necessarily full rank, but we assume that its rank is a constant, $m\leq n$, as a function of t. $C(t)$ and $G(t)$ are T-periodic. The homogeneous system corresponding to (1) is given by

$$\frac{d}{dt}\left(C(t)x\right)+G(t)x=0 \tag{2}$$

Solution and related subspaces

When $C(t)$ is rank deficient, (2) does *not* have solutions for all initial conditions $x(0)=x_0\in\mathbb{R}^n$. We assume that the DAEs we are dealing with are index-1 [2]. Then, the solutions of the homogeneous system (2) lie in an m-dimensional subspace defined by [2]

$$S(t)=\left\{z\in\mathbb{R}^n:\left(G(t)+\dot{C}(t)\right)z\in\operatorname{im}C(t)\right\} \tag{3}$$

Also, every $x(t)\in S(t)$ is a solution of (2) [2]. Let $N(t)$ be the null space of $C(t)$:

$$N(t)=\ker C(t) \tag{4}$$

which is an $n-m=k$-dimensional subspace. For index-1 DAEs, we have [2, 3] $S(t)\cap N(t)=\{0\}$ and

$$S(t)\oplus N(t)=\mathbb{R}^n \tag{5}$$

[1] Note that the time derivative operates on the product $C(t)x$, not on x only. It will become clear in Section 3 why we use this form.

where $\oplus$ denotes *direct sum decomposition*. For our purposes, it suffices to know that (5) is equivalent to the following: If $Z(t) = \{z_1(t), z_2(t), \ldots, z_m(t)\}$ is a basis for $S(t)$, and $W(t) = \{w_1(t), w_2(t), \ldots, w_k(t)\}$ is a basis for $N(t)$, then $Z(t) \cup W(t)$ is a basis for $\mathbb{R}^n$.

Adjoint system and related subspaces

Before we discuss the forms of the solutions of (2) and (1), we would like to introduce the *adjoint* or *dual* system corresponding to (2), and the related subspaces. The adjoint system corresponding to (2) is given by

$$C^T(t)\frac{d}{dt}y - G^T(t)y = 0 \tag{6}$$

Note that the time derivative operates on y only, not on the product $C^T(t)y$, in contrast with (2). It will become clear shortly why (6) is the form for the adjoint of (2). If $y(t)$ is a solution of (6) and $x(t)$ is a solution of (2), then we have

$$\begin{aligned}\frac{d}{dt}\left(y^T(t)C(t)x(t)\right) &= \left(\frac{d}{dt}y^T(t)\right)C(t)x(t) + y^T(t)\frac{d}{dt}\left(C(t)x(t)\right)\\ &= y^T(t)G(t)x(t) - y^T(t)G(t)x(t)\\ &= 0\end{aligned}$$

Thus $y^T(t)C(t)x(t) = y^T(0)C(0)x(0) \quad$ for all $t \geq 0$. Let

$$S^T(t) = \{z \in \mathbb{R}^n : G^T(t)z \in \operatorname{im} C^T(t)\} \tag{7}$$

and

$$N^T(t) = \ker C^T(t) \tag{8}$$

Then $S^T(t) \cap N^T(t) = \{0\}$ and $S^T(t) \oplus N^T(t) = \mathbb{R}^n$.

State-transition matrix and the solution

Having introduced the adjoint system for (2), we now consider the state-transition matrix and the solutions for (2) and (1).

Theorem 2.1 *The solution ϕ of (2) satisfying the initial condition $x(0) = x_0 \in S(0)$ is given by*

$$\phi(t, x_0) = \Phi(t, 0)x_0 \tag{9}$$

where the "state transition matrix" $\Phi(t,s)$ is given by[2]

$$\Phi(t,s) = U(t)D(t-s)V(s)C(s) \tag{10}$$

where

$$D(t-s) = diag[\exp(\mu_1(t-s)), \ldots, \exp(\mu_m(t-s)), \underbrace{0, \ldots, 0}_{k}]$$

$U(t) : n \times n$ and $V(t) : n \times n$ are both T-periodic and nonsingular (for all t), and satisfy

$$V(t)C(t)U(t) = \begin{bmatrix} I_m & 0 \\ 0 & 0 \end{bmatrix} \tag{11}$$

μ_i are called the characteristic (Floquet) exponents of (2), and $\lambda_i = \exp(\mu_i T)$ are called the (Floquet) characteristic multipliers. Note that (2) has $k = n - m$ Floquet multipliers that are 0.

Let $u_i(t)$ be the columns of $U(t)$, and $v_i^T(t)$ be the rows of $V(t)$:

$$U(t) = [u_1(t), \ldots, u_m(t), u_{m+1}(t), \ldots, u_n(t)] \tag{12}$$

$$V^T(t) = [v_1(t), \ldots, v_m(t), v_{m+1}(t), \ldots, v_n(t)] \tag{13}$$

$\{u_1(t), \ldots, u_m(t)\}$ is a basis for $S(t)$, and $\{u_{m+1}(t), \ldots, u_n(t)\}$ is a basis for $N(t)$. Similarly, $\{v_1(t), \ldots, v_m(t)\}$ is a basis for $S^T(t)$, and $\{v_{m+1}(t), \ldots, v_n(t)\}$ is a basis for $N^T(t)$. For $1 \leq i \leq m$, $x(t) = u_i(t)\exp(\mu_i t)$ is a solution of (2) with the initial condition $x(0) = u_i(0)$. Similarly, for $1 \leq i \leq m$, $y(t) = v_i(t)\exp(-\mu_i t)$ is a solution of (6) with the initial condition $y(0) = v_i(0)$.

[2] Authors in [3] derive a similar result for the state-transition matrix of a DAE system.

Remark 2.1 *The following orthogonality/biorthogonality conditions hold:*

$$v_j^T(t)C(t)u_i(t) = \delta_{ij} \qquad i = 1, \ldots, m \;\; j = 1, \ldots, m \tag{14}$$

$$v_j^T(t)C(t)u_i(t) = 0 \qquad i = 1, \ldots, m \;\; j = m+1, \ldots, n \tag{15}$$

$$v_j^T(t)G(t)u_i(t) = 0 \qquad i = m+1, \ldots, n \;\; j = 1, \ldots, m \tag{16}$$

(14) and (15) follow from (11). (16) follows from the fact that $v_i(t)\exp(-\mu_i t)$, $j = 1, \ldots, m$ is a solution of (6), and $u_i(t)$, $i = m+1, \ldots, n$ is in the null space $N(t)$ of $C(t)$.

The state transition matrix $\Phi(t,s)$ in (10) can be rewritten as

$$\Phi(t,s) = \sum_{i=1}^{m} \exp(\mu_i(t-s))u_i(t)v_i^T(s)C(s) \tag{17}$$

Theorem 2.2 *The solution ϕ of (1) satisfying the initial condition $x(0) = x_0 \in S(0)$ (for $b(0) = 0$) is given by*

$$\phi(t, x_0) = \Phi(t,0)x_0 + \int_0^t \Psi(t,s)b(s)\mathrm{d}s + \Gamma(t)b(t) \tag{18}$$

where

$$\Psi(t,s) = U(t)D(t-s)V(s) \tag{19}$$

and $\Gamma(t) : n \times n$ is a T-periodic matrix of rank k which satisfies

$$\Gamma(t)C(t)[u_1(t), \ldots, u_m(t)] = 0 \tag{20}$$

i.e., the null space of $\Gamma(t)$ is spanned by $\{C(t)u_1(t), \ldots, C(t)u_m(t)\}$.

From (10) and (19), the solutions of the homogeneous system (2) and the inhomogeneous system (1) are respectively given by

$$x_H(t) = \sum_{i=1}^{m} \exp(\mu_i t)u_i(t)v_i^T(0)C(0)x(0)$$

$$x_{IH}(t) = x_H(t) + \sum_{i=1}^{m} u_i(t)\int_0^t \exp(\mu_i(t-s))v_i^T(s)b(s)\mathrm{d}s + \Gamma(t)b(t)$$

If the initial condition $x(0) = x_0$ is not in $S(0)$, i.e., if it is not a consistent initial condition for (2), then $x(t) = \Phi(t,0)x_0$ is *still* a solution of (2), but it does not satisfy $x(0) = x_0$. Any $x_0 \in \mathbb{R}^n$ can be written as $x_0 = x_{0eff} + x_{0N}$ where $x_{0eff} \in S(0)$ and $x_{0N} \in N(0)$, which follows from (5). Then

$$\Phi(t,0)x_0 = U(t)D(t)V(0)C(0)x_0 = \Phi(t,0)x_{0eff}$$

since $C(0)x_0 = C(0)x_{0eff}$. Hence, $x(t) = \Phi(t,0)x_0$ is a solution of (2) satisfying the *effective* initial condition $x(0) = x_{0eff}$.

State-transition matrix for the adjoint system

The state-transition matrix $\Omega(t,s)$ for the adjoint system (6) is *not* simply given by $\Phi^T(s,t)$ in terms of the state transition matrix $\Phi(t,s) = U(t)D(t-s)V(s)C(s)$ for (2), as it would be the case for ODEs. Instead, it is given by

$$\begin{aligned}\Omega(t,s) &= V^T(t)D(s-t)U^T(s)C^T(s)\\ &= \sum_{i=1}^{m} \exp(-\mu_i(t-s))v_i(t)u_i^T(s)C^T(s)\end{aligned}$$

Monodromy matrix

We define the monodromy matrix for (2) as $\Phi(T,0)$, and it is given by

$$\Phi(T,0) = \sum_{i=1}^{m} \exp(\mu_i T)u_i(T)v_i^T(0)C(0) = \sum_{i=1}^{m} \exp(\mu_i T)u_i(0)v_i^T(0)C(0)$$

$u_i(0)$ for $i = 1, \ldots, m$ are the eigenvectors of the monodromy matrix $\Phi(T,0)$ with corresponding eigenvalues $\exp(\mu_i T)$, and $u_i(0)$ for

$i = m+1, \ldots, n$ are the eigenvectors of the monodromy matrix $\Phi(T,0)$ corresponding to the k-fold eigenvalue 0. $v_i(0)$ are *not* the eigenvectors of the *transposed* monodromy matrix $\Phi(T,0)^T$. Here, we must consider the monodromy matrix $\Omega(T,0)$ for the adjoint system (6), which is given by

$$\Omega(T,0) = \sum_{i=1}^{m} \exp(-\mu_i T) v_i(0) u_i^T(0) C^T(0) \tag{21}$$

Now, $v_i(0)$ for $i = 1, \ldots, m$ are the eigenvectors of the monodromy matrix $\Omega(T,0)$ with corresponding eigenvalues $\exp(-\mu_i T)$, and $v_i(0)$ for $i = m+1, \ldots, n$ are the eigenvectors of the monodromy matrix $\Omega(T,0)$ corresponding to the k-fold eigenvalue 0.

Numerical computation of the monodromy matrix

The eigenvalues of the monodromy matrix determine the stability of (2) [4, 5]. Hence, one would like to calculate the monodromy matrix and its eigenvalues. Authors in [5] define a *reduced* monodromy matrix for (2) as a *nonsingular* $m \times m$ matrix, as opposed to the monodromy matrix we defined which is $n \times n$ and has k eigenvalues equal to 0. The monodromy matrix they define has the same eigenvalues as the one we define, except for the k-fold eigenvalue 0. For the numerical computation of the reduced monodromy matrix, as proposed by the authors in [5], one needs to calculate m linearly independent consistent initial conditions for (2). With our definition, we avoid having to compute m linearly independent consistent initial conditions for (2). Instead, we integrate (2) with an *effective* matrix (rank m) initial condition $X_{0eff} : n \times n$ (columns of which are consistent initial conditions for (2)) from $t = 0$ to $t = T$ to calculate the monodromy matrix as follows: In numerical integration of (2), we set the initial condition $X(0) = I_n$, the n-dimensional identity matrix. From (5), we can write $I_n = X_{0eff} + X_{kerC}$ where the columns of X_{0eff} lie in $S(0)$ of (3)[3], and the columns of X_{kerC} lie in $N(0)$ (null space of $C(0)$). $X(0) = X_{0eff}$ is effectively realized during numerical integration by

$$C(0) I_n = C(0) X_{0eff} + C(0) X_{kerC} = C(0) X_{0eff}$$

Note that during the numerical integration of (2), one does not need to calculate X_{0eff} itself, but only $C(0)X_{0eff} = C(0)I_n$. The numerical integration of (2) is started with an order 1 method (i.e., backward Euler) at t=0 that requires only $C(0)X(0)$ to compute the $X(t)$ at the first time step. If one would like to obtain the effective initial condition X_{0eff}, a backwards step in time (with the same time step) can be taken after the first forward time step is computed.[4] This is a much more efficient way of computing consistent initial conditions for (2) then the one used in [5].

3 Perturbation analysis for autonomous DAEs

Consider the system of autonomous DAEs:

$$\frac{d}{dt} q(x) + g(x) = 0 \tag{22}$$

We assume that (22) has an asymptotically orbitally stable periodic solution $x_s(t)$ with period T, i.e., a stable limit cycle in the solution space. Hence

$$\frac{d}{dt} q(x_s) + g(x_s) = 0 \tag{23}$$

Let us take the derivative of both sides of (23) with respect to t:

$$\frac{d}{dt}\left(\frac{d}{dx} q(x)\Big|_{x=x_s} \dot{x}_s \right) + \frac{d}{dx} g(x)\Big|_{x=x_s} \dot{x}_s = 0 \tag{24}$$

Thus, $\dot{x}_s(t)$ is a T-periodic solution of the LPTV system of DAEs

$$\frac{d}{dt}\left(C(t)\,x\right) + G(t)\,x = 0 \tag{25}$$

where

$$C(t) = \frac{d}{dx} q(x)\Big|_{x=x_s} \tag{26}$$

$$G(t) = \frac{d}{dx} g(x)\Big|_{x=x_s} \tag{27}$$

Let $\Phi(t,s)$ be the state transition matrix of (25). Since (25) has a T-periodic solution $\dot{x}_s(t)$, we can choose, without loss of generality,

$$u_1(t) = -\dot{x}_s(t) \tag{28}$$

and

$$\lambda_1 = \exp(\mu_1 T) = 1 \tag{29}$$

in the representation of $\Phi(t,s)$ in (17). Hence, one of the Floquet (characteristic) multipliers of (25) is 1. One can show that if the remaining $m-1$ Floquet multipliers have magnitudes less than 1, i.e.,

$$|\lambda_i| = |\exp(\mu_i T)| < 1 \quad i = 2, \ldots, m \tag{30}$$

then $x_s(t)$ is an asymptotically orbitally stable solution of (22).

Lemma 3.1 *If $x_s(t)$ is a solution of (22), then $x_s(t+\alpha(t))$ is a solution of*

$$\frac{d}{dt} q(x) + g(x) + c_1(t) C(t+\alpha(t)) u_1(t+\alpha(t)) = 0 \tag{31}$$

where the scalars $c_1(t)$ and $\alpha(t)$ satisfy

$$\frac{d}{dt}\alpha(t) = c_1(t)$$
$$c_1(t) = 0 \quad for \quad t < 0 \qquad alpha(0) = 0$$

Now, consider a small, additive, state-dependent perturbation of the form $B(x)b(t)$ to (22) (where $B(\cdot) : \mathbb{R}^n \to \mathbb{R}^{n\times p}$ and $b(\cdot) : \mathbb{R} \to \mathbb{R}^p$):

$$\frac{d}{dt} q(x) + g(x) + B(x)b(t) = 0 \tag{32}$$

Next, we decompose the (small) perturbation $B(x)b(t)$ into its components using

$$\{C(t+\alpha(t))u_1(t+\alpha(t)), \ldots, C(t+\alpha(t))u_m(t+\alpha(t)),$$
$$G(t+\alpha(t))u_{m+1}(t+\alpha(t)) \ldots, G(t+\alpha(t))u_n(t+\alpha(t))\}$$

as the basis[5], where $u_i(t)$ are the columns of $U(t)$ of Section 2

$$B(x)b(t) = \sum_{i=1}^{m} c_i(x,\alpha(t),t) C(t+\alpha(t)) u_i(t+\alpha(t)) + \sum_{i=m+1}^{n} c_i(x,\alpha(t),t) G(t+\alpha(t)) u_i(t+\alpha(t)) \tag{33}$$

where the coefficients $c_i(x,\alpha(t),t)$, $1 \le i \le m$ are given by

$$c_i(x,\alpha(t),t) = v_i^T(t+\alpha(t)) B(x) b(t) \quad \text{for} \quad 1 \le i \le m \tag{34}$$

which was obtained using the orthogonality/biorthogonality relationships in (14) and (16). We distinguish the component in (33) along $C(t+\alpha(t))u_1(t+\alpha(t)) = -C(t+\alpha(t))\dot{x}_s(t+\alpha(t))$ from the rest:

$$b_1(x,t) = c_1(x,\alpha(t),t) C(t+\alpha(t)) u_1(t+\alpha(t))$$
$$\tilde{b}(x,t) = B(x)b(t) - b_1(x,t)$$

[3] They also span $S(0)$, since the columns of I_n are linearly independent.

[4] The author would like to thank Hans Georg Brachtendorf for pointing this out.

[5] Recall that the columns of $U(t)$ form a basis for $\mathbb{R}^n$ for index-1 DAEs. It can be shown that $\{C(t+\alpha(t))u_1(t+\alpha(t)), \ldots, C(t+\alpha(t))u_m(t+\alpha(t)), G(t+\alpha(t))u_{m+1}(t+\alpha(t)) \ldots, G(t+\alpha(t))u_n(t+\alpha(t))\}$ also forms a basis for $\mathbb{R}^n$ for the index-1 DAE case.

Theorem 3.1

1. $x_s(t+\alpha(t))$ *solves*

$$\frac{d}{dt}q(x)+g(x)+b_1(x,t)=\frac{d}{dt}q(x)+g(x)+$$
$$v_1^T(t+\alpha(t))B(x)b(t)C(t+\alpha(t))u_1(t+\alpha(t))=0$$

where

$$\frac{d}{dt}\alpha(t)=v_1^T(t+\alpha(t))B(x_s(t+\alpha(t))b(t) \quad \alpha(0)=0 \qquad (35)$$

2. $x_s(t+\alpha(t))+z(t)$ *solves*

$$\frac{d}{dt}q(x)+g(x)+B(x)b(t)=0 \qquad (36)$$

where $z(t)$ does not *grow without bound and it indeed stays small (within a factor of $b(t)$). If $b(t)=0,\ t>t_c$ for some $t_c>0$, then $z(t)\to 0$ as $t\to\infty$, and $x_s(t+\alpha(t_c))$ solves (36) for $t\to\infty$.*

We considered the perturbed system of DAEs in (32), and obtained the following results: The unperturbed oscillator's periodic response $x_s(t)$ is modified to $x_s(t+\alpha(t))+z(t)$ by the perturbation, where $\alpha(t)$ is a changing time shift, or *phase deviation*, in the periodic output of the unperturbed oscillator, $z(t)$ is an additive component, which we term the *orbital deviation*, to the phase-shifted oscillator waveform. $\alpha(t)$ and $z(t)$ are such that: $\alpha(t)$ will, in general, keep increasing with time even if the perturbation $b(t)$ is always small, and if the perturbation is removed, $\alpha(t)$ will settle to a constant value. The orbital deviation $z(t)$, on the other hand, will always remain small (within a bounded factor of $b(t)$), and if the perturbation is removed, $z(t)$ will decay to zero. Furthermore, we derived a *nonlinear differential equation* (35) for the phase deviation $\alpha(t)$.

Numerical methods

For perturbation analysis and phase noise/timing jitter characterizations of an oscillator, one needs to calculate the steady-state periodic solution $x_s(t)$ and the periodic vector $v_1(t)$ that appears in (35). Below, we describe the numerical computation of $v_1(t)$.

1. Compute the large-signal periodic steady-state solution $x_s(t)$ for $0\le t\le T$ by numerically integrating (22), possibly using a technique such as the shooting method [6].
2. Compute the monodromy matrix $\Omega(-T,0)$[6] in (21) by numerically integrating

$$C^T(t)\frac{d}{dt}Y-G^T(t)Y=0 \quad Y(0)=I_n \qquad (37)$$

from 0 to $-T$, backwards in time, where $C(t)$ and $G(t)$ are defined in (26). Note that $\Omega(-T,0)=Y(-T)$. Note that it is not numerically stable to calculate $\Omega(T,0)$ by integrating (37) *forward* in time. Since $C(t)$ is not full rank, in general, $Y(0)=I_n$ can not be realized in solving (37). Please see the discussion at the end of Section 2.

3. Compute $u_1(0)$ using $u_1(0)=-\dot{x}_s(0)$.
4. $v_1(0)$ is an eigenvector of $\Omega(-T,0)$ corresponding to the eigenvalue 1. To compute $v_1(0)$, first compute an eigenvector of $\Omega(-T,0)$ corresponding to the eigenvalue 1, then scale this eigenvector so that

$$v_1(0)^T C(0)\,u_1(0)=1 \qquad (38)$$

is satisfied. For some oscillators (encountered quite often in practice), there can be "many" other eigenvalues of $\Omega(-T,0)$ with magnitudes very close to 1, and they may not be *numerically* distinguishable from the eigenvalue that is theoretically equal to 1. In this case, to choose the correct eigenvector of $\Omega(-T,0)$ as $v_1(0)$, calculate the inner products of these eigenvectors with $C(0)\dot{x}_s(0)$ and choose the vector which has the largest inner product. Theoretically, the inner products of the "wrong" eigenvectors with $C(0)\dot{x}_s(0)$ are 0.

5. Compute the periodic vector $v_1(t)$ for $0\le t\le T$ by numerically integrating the adjoint system backwards in time

$$C^T(t)\frac{d}{dt}y-G^T(t)y=0 \qquad (39)$$

using $v_1(0)=v_1(T)$ as the initial condition. Note that $v_1(t)$ is a periodic steady-state solution of (39) corresponding to the Floquet multiplier that is equal to 1. It is not numerically stable to calculate $v_1(t)$ by numerically integrating (39) *forward* in time.

In implementing the above algorithm, one can increase the efficiency by saving LU factored matrices that need to be calculated in Step 2 and reuse them in Step 5. One can also avoid calculating the full $n\times n$ monodromy matrix $\Omega(-T,0)$ explicitly, and use iterative methods (which require only the computation of products of $\Omega(-T,0)$ with some vectors) at Step 4 to calculate the eigenvector of $\Omega(-T,0)$ that corresponds to the eigenvalue 1.

4 Stochastic characterization of the phase deviation with colored noise sources

We now find the probabilistic characterisation of the phase deviation $\alpha(t)$ (which satisfies the differential equation (35)) as a stochastic process when the perturbation $b(t)$ is a (one-dimensional) stationary, zero-mean ($\mathtt{E}\,[b(t)]=0$), Gaussian colored stochastic process[7]. Let $R_N(\tau)$ be the autocovariance function, and $S_N(f)$ be the power spectral density, of the stationary Gaussian stochastic process $b(t)$:

$$R_N(\tau) = \mathtt{E}\,[b(t+\tau/2)\,b(t-\tau/2)] \qquad (40)$$

$$S_N(f) = \mathtt{F}\,\{R_N(\tau)\}=\int_{-\infty}^{\infty}R_N(\tau)\exp(-j2\pi f\tau)\,\mathrm{d}\tau \qquad (41)$$

Note that $R_N(\tau)$ is a real and even function of τ. Let $v(t)=v_1^T(t)B(x_s(t))$, which is a scalar (both $v_1(.)$ and $B(.)$ are vectors) that is periodic in t with period T. Hence, (35) becomes

$$\frac{\mathrm{d}\alpha(t)}{\mathrm{d}t}=v(t+\alpha(t))\,b(t), \quad \alpha(0)=0 \qquad (42)$$

In this section, we will follow the below procedure to find an adequate probabilistic characterization of the phase deviation $\alpha(t)$ due to the colored noise source $b(t)$ for our purposes:

1. We first derive a *partial integro-differential equation* for the time-varying marginal *probability density function* (PDF) $p_\alpha(\eta,t)$ of $\alpha(t)$ defined as

$$p_\alpha(\eta,t)=\frac{\partial\mathtt{P}\,(\alpha(t)\le\eta)}{\partial\eta} \quad t\ge 0 \qquad (43)$$

where $\mathtt{P}\,(.)$ denotes the *probability measure*.

2. We then show that the PDF of a Gaussian random variable, "asymptotically" with t, solves this partial integro-differential equation. A Gaussian PDF is completely characterised by the mean and the variance. We show that $\alpha(t)$ becomes (under some conditions on $R_N(\tau)$ or $S_N(f)$), for "large" (to be concretized) t, a Gaussian random variable with a constant mean and a variance that is given by

$$\mathrm{var}(\alpha(t))=\beta\int_0^t\int_0^t R_N(t_1-t_2)\,\mathrm{d}t_1\,\mathrm{d}t_2 \qquad (44)$$

Theorem 4.1 *If $b(t)$ is a stationary, zero-mean, Gaussian stochastic process with autocovariance function $R_N(\tau)$, and if $\alpha(t)$ satisfies (42), then the time-varying marginal PDF $p_\alpha(\eta,t)$ of α satisfies*

$$\frac{\partial p_\alpha(\eta,t)}{\partial t}=-\frac{\partial}{\partial\eta}\left(\frac{\partial v(t+\eta)}{\partial\eta}\int_0^t v(\tau+\eta)R_N(t-\tau)\,p_\alpha(\eta,t)\,d\tau\right)+$$
$$\frac{\partial^2}{\partial\eta^2}\left(v(t+\eta)\int_0^t v(\tau+\eta)R_N(t-\tau)\,p_\alpha(\eta,t)\,d\tau\right) \qquad (45)$$

[6] Note the minus sign in front of T.

[7] The extension to the case when $b(t)$ is a vector of uncorrelated white and colored noise sources is discussed in Section 7. Noise sources in electronic devices usually have independent physical origin, and hence they are modeled as uncorrelated stochastic processes. Hence, we consider uncorrelated noise sources. However, the generalization of our results to correlated noise sources is trivial.

with the initial/boundary condition for $t = 0$

$$p_\alpha(\eta, 0) = \delta(\eta) \tag{46}$$

i.e., $\mathrm{E}\left[\alpha(0)\right] = 0$ *and* $\mathrm{E}\left[\alpha^2(0)\right] = 0$.

The partial integro-differential equation (45) for the time-varying marginal PDF $p_\alpha(\eta, t)$ of $\alpha(t)$ is a generalization of a partial differential equation known as the *Fokker-Planck equation* [7, 8] derived for the PDF of $\alpha(t)$ satisfying (42) when $b(t)$ is a white noise process, which is given below

$$\begin{aligned}\frac{\partial p_\alpha(\eta,t)}{\partial t} = &-\frac{\partial}{\partial \eta}\left(\lambda \frac{\partial v(t+\eta)}{\partial \eta} v(t+\eta) p_\alpha(\eta,t)\right) + \\ &\frac{1}{2}\frac{\partial^2}{\partial \eta^2}\left(v^2(t+\eta) p_\alpha(\eta,t)\right)\end{aligned} \tag{47}$$

where $0 \le \lambda \le 1$ depends on the definition of the stochastic integral [7] used to interpret the stochastic differential equation in (42) with $b(t)$ as a white noise process. If $b(t)$ is a white noise process, then $\alpha(t)$ is a Markov process. However, when $b(t)$ is colored, $\alpha(t)$, in general, is not Markovian. (47) is valid for any initial/boundary condition. On the other hand, (45) is valid only for initial/boundary conditions of the type

$$p_\alpha(\eta, 0) = \delta(\eta - \alpha_0) \tag{48}$$

for some α_0.

We would like to solve (45) for $p_\alpha(\eta, t)$. We do this by first solving for the *characteristic function* $F(\omega, t)$ of $\alpha(t)$, which is defined by

$$F(\omega, t) = \mathrm{E}\left[\exp\left(j\omega\alpha(t)\right)\right] = \int_{-\infty}^{\infty} \exp\left(j\omega\eta\right) p_\alpha(\eta, t) \mathrm{d}\eta$$

$v(t)$ is T-periodic, hence we can expand $v(t)$ into its Fourier series:

$$v(t) = \sum_{i=-\infty}^{\infty} V_i \exp(ji\omega_0 t), \qquad \omega_0 = \frac{2\pi}{T}$$

Lemma 4.1 *The characteristic function of $\alpha(t)$, $F(\omega, t)$, satisfies*

$$\begin{aligned}\frac{\partial F(\omega,t)}{\partial t} = &\sum_{i=-\infty}^{\infty}\sum_{k=-\infty}^{\infty} V_i V_k^* \exp(j\omega_0 i t)\left(-\omega_0 i\omega - \omega^2\right) \\ &\int_0^t R_N(t-\tau)\exp(-j\omega_0 k\tau) F(\omega_0(i-k)+\omega, t) d\tau\end{aligned} \tag{49}$$

where $*$ denotes complex conjugation.

Theorem 4.2 *(49) has a solution that becomes (with time) the characteristic function of a Gaussian random variable:*

$$F(\omega, t) = \exp\left(j\omega\mu(t) - \frac{\omega^2\sigma^2(t)}{2}\right) \tag{50}$$

solves (49) for t large enough such that

$$\exp\left(-\frac{1}{2}\omega_0^2 (i-k)^2 \sigma^2(t)\right) \approx \begin{cases} 1 & i = k \\ 0 & i \ne k \end{cases} \tag{51}$$

where

$$\frac{d\mu(t)}{dt} = \sum_{i=-\infty}^{\infty} j\omega_0 i \left|V_i\right|^2 \int_0^t R_N(t-\tau)\exp\left(j\omega_0 i(t-\tau)\right) d\tau \tag{52}$$

$$\frac{d\sigma^2(t)}{dt} = \sum_{i=-\infty}^{\infty} 2\left|V_i\right|^2 \int_0^t R_N(t-\tau)\exp\left(j\omega_0 i(t-\tau)\right) d\tau \tag{53}$$

Assumption 4.1

$$\int_0^t R_N(t-\tau)\exp\left(j\omega_0 i(t-\tau)\right) d\tau \approx \begin{cases} \int_0^t R_N(t-\tau) d\tau & i = 0 \\ 0 & i \ne 0 \end{cases} \tag{54}$$

This is satisfied when the *bandwidth* of the colored noise source is much *less* than the oscillation frequency ω_0, or equivalently, the *correlation width* of the colored noise source in time is much *larger* than the oscillation period $T = 2\pi/\omega_0$. We will further comment on this condition in Section 5, where we discuss the models for burst and $1/f$ noise. With (54), (52) and (53) become

$$\frac{\mathrm{d}\mu(t)}{\mathrm{d}t} = 0 \qquad \frac{\mathrm{d}\sigma^2(t)}{\mathrm{d}t} = 2\left|V_0\right|^2 \int_0^t R_N(t-\tau)\mathrm{d}\tau \tag{55}$$

From (55)

$$\sigma^2(t) = 2\left|V_0\right|^2 \int_0^t \int_0^{t_2} R_N(t_2 - t_1)\mathrm{d}t_1\mathrm{d}t_2 \tag{56}$$

follows trivially. Since, the autocovariance $R_N(\tau)$ is an even function of τ, (56) can be rewritten as

$$\sigma^2(t) = \left|V_0\right|^2 \int_0^t \int_0^t R_N(t_2 - t_1)\mathrm{d}t_1\mathrm{d}t_2 \tag{57}$$

Thus, we obtained (44).

Lemma 4.2 *The variance $\sigma^2(t)$ of $\alpha(t)$ in (56) can be rewritten with a single integral as follows:*

$$\sigma^2(t) = 2\left|V_0\right|^2 \int_0^t (t-\tau) R_N(\tau) d\tau \tag{58}$$

It can also be expressed in terms of the spectral density of the colored noise source $b(t)$ as follows:

$$\sigma^2(t) = 2\left|V_0\right|^2 \int_{-\infty}^{\infty} S_N(f) \frac{(1 - \exp(j2\pi ft))}{4\pi^2 f^2} df \tag{59}$$

5 Models for burst (popcorn) and $1/f$ (flicker) noise

Burst noise

The source of burst noise is not fully understood, although it has been shown to be related to the presence of heavy-metal ion contamination [9]. For practical purposes, burst noise is usually modeled with a colored stochastic process with Lorentzian spectrum, i.e., the spectral density of a burst noise source is given by

$$S_{burst}(f) = K \frac{I^a}{1 + \left(\frac{f}{f_c}\right)^2} \tag{60}$$

where K is a constant for a particular device, I is the current through the device, a is a constant in the range 0.5 to 2, and f_c is the 3 dB bandwidth of the Lorentzian spectrum [9]. Burst noise often occurs with multiple time constants, i.e., the spectral density is the summation of several Lorentzian spectra as given by (60) with different 3 dB bandwidths.

A stationary colored stochastic process with spectral density

$$S_{Nburst}(f) = \frac{\gamma^2}{\gamma^2 + (2\pi f)^2} \tag{61}$$

has the autocorrelation function

$$R_{Nburst}(\tau) = \frac{\gamma}{2}\exp\left(-\gamma|\tau|\right) \tag{62}$$

If the 3 dB bandwidth γ of (61) is much less than the oscillation frequency ω_0, or equivalently, the correlation width $1/\gamma$ of (62) is much larger than the oscillation period $T = 2\pi/\omega_0$, then (54) is satisfied.

$1/f$ noise

$1/f$ noise is ubiquitous in all physical systems (as a matter of fact, in all kinds of systems). The origins of $1/f$ noise is varied. In IC devices, it is believed to be caused mainly by traps associated with contamination and crystal defects, which capture and release charge carriers in a random fashion, and the time constants associated with

this process give rise to a noise signal with energy concentrated at low frequencies. For practical purposes it is modeled with a "stationary" and colored stochastic process with a spectral density given by

$$S_{1/f}(f) = K\frac{I^a}{f} \tag{63}$$

where K is a constant for a particular device, I is the current through the device, and a is a constant in the range 0.5 to 2. There is a lot of controversy both about the origins and modeling of $1/f$ noise. The spectral density in (63) is not a well-defined spectral density for a stationary stochastic process: It blows up at $f = 0$. Keshner in [10] argues that $1/f$ noise is *really* a nonstationary process, and when one tries to model it as a stationary process, this nonphysical artifact arises. We are not going to dwell into this further, which would fill up pages and would not be too useful other than creating a lot of confusion. Instead, we will "postulate" a well-defined *stationary* stochastic process model for $1/f$ noise: We will introduce a cut-off frequency in (63), below which the spectrum deviates from $1/f$ and attains a finite value at $f = 0$. To do this, we use the following integral representation [11]

$$\frac{1}{|f|} = 4\int_0^\infty \frac{1}{\gamma^2 + (2\pi f)^2}\mathrm{d}\gamma \tag{64}$$

We introduce the cut-off frequency γ_c in (64), and use

$$\begin{aligned} S_{N1/f}(f) &= 4\int_{\gamma_c}^\infty \frac{1}{\gamma^2 + (2\pi f)^2}\mathrm{d}\gamma & (65)\\ &= \frac{1}{|f|} - 4\frac{\arctan\left(\frac{\gamma_c}{2\pi f}\right)}{2\pi f} & (66)\end{aligned}$$

for the spectral density of a stationary stochastic process that models $1/f$ noise. The spectral density in (65) has a finite value at $f = 0$:

$$S_{N1/f}(0) = \frac{4}{\gamma_c} \tag{67}$$

The autocorrelation function that corresponds to the spectral density in (65) is given by

$$R_{N1/f}(\tau) = 2E_1(\gamma_c|\tau|) \tag{68}$$

where the exponential integral $E_1(z)$ is defined as

$$E_1(t) = \int_1^\infty \frac{\exp(-tz)}{z}\mathrm{d}z$$

The power in a $1/f$ noise source modeled with a stochastic process with the spectral density (65) is concentrated at low frequencies, frequencies much less than the oscillation frequency for practical oscillators. Hence, (54) is satisfied for $1/f$ noise sources.

6 Spectrum of an oscillator with phase noise due to colored noise sources

Having obtained the stochastic characterization of $\alpha(t)$ due to a colored noise source in Section 4, we now compute the spectral density of the oscillator output, i.e., $x_s(t+\alpha(t))$. We first obtain an expression for the non-stationary autocovariance function $R(t,\tau)$ of $x_s(t+\alpha(t))$. Next, we demonstrate that the autocovariance is independent of t for "large" time. Finally, we calculate the spectral density of $x_s(t+\alpha(t))$ by taking the Fourier transform of the stationary autocovariance function for $x_s(t+\alpha(t))$.

We start by calculating the autocovariance function of $x_s(t+\alpha(t))$, given by

$$R_V(t,\tau) = \mathtt{E}\left[x_s(t+\alpha(t))\,x_s^*(t+\tau+\alpha(t+\tau))\right] \tag{69}$$

Definition 6.1 *Define X_i to be the Fourier coefficients of $x_s(t)$:*

$$x_s(t) = \sum_{i=-\infty}^{\infty} X_i \exp(ji\omega_0 t)$$

The following simple Lemma establishes the basic form of the autocovariance:

Lemma 6.1

$$\begin{aligned} R_V(t,\tau) = \sum_{i=-\infty}^{\infty}\sum_{k=-\infty}^{\infty} X_i X_k^* \exp(j(i-k)\omega_0 t)\exp(-jk\omega_0\tau)\\ \mathtt{E}\left[\exp(j\omega_0(i\alpha(t)-k\alpha(t+\tau)))\right]\end{aligned} \tag{70}$$

The expectation in (70), i.e., $\mathtt{E}\left[\exp(j\omega_0(i\alpha(t)-k\alpha(t+\tau)))\right]$ is the characteristic function of $i\alpha(t)-k\alpha(t+\tau)$. This expectation is independent of t for large time as established by the following theorem:

Theorem 6.1 *If t is large enough such that*

$$\exp\left(-\frac{1}{2}\omega_0^2(i-k)^2\sigma^2(t)\right) \approx \begin{cases} 1 & i=k \\ 0 & i\neq k\end{cases} \tag{71}$$

then $i\alpha(t)-k\alpha(t+\tau)$ is a Gaussian random variable and its characteristic function, which is independent of t, is given by

$$\mathtt{E}\left[\exp(j\omega_0(i\alpha(t)-k\alpha(t+\tau)))\right] \approx \begin{cases} 0 & i\neq k \\ \exp\left(-\frac{1}{2}\omega_0^2 i^2\sigma^2(|\tau|)\right) & i=k\end{cases} \tag{72}$$

where $\sigma^2(t)$ is as in (57), (58) or (59). Note that the condition (71) is same as the condition (51) in Theorem 4.2.

We now obtain the stationary autocovariance function:

Corollary 6.1

$$R_V(\tau) = \sum_{i=-\infty}^{\infty} X_i X_i^* \exp(-ji\omega_0\tau)\exp\left(-\frac{1}{2}\omega_0^2 i^2\sigma^2(|\tau|)\right) \tag{73}$$

To obtain the spectral density of $x_s(t+\alpha(t))$, we calculate the Fourier transform of (73):

$$S_V(f) = \sum_{i=-\infty}^{\infty} X_i X_i^*\, S_i(f+i f_0) \tag{74}$$

where $\omega_0 = 2\pi f_0$ and

$$\begin{aligned} S_i(f) &= \mathtt{F}\left\{R_i(\tau)\right\} & (75)\\ &= \mathtt{F}\left\{\exp\left(-\frac{1}{2}\omega_0^2 i^2\sigma^2(|\tau|)\right)\right\} & (76)\end{aligned}$$

The Fourier transform in (76) does not have a simple closed form. Mullen and Middleton in [12] calculate various limiting forms for this Fourier transform through approximating series expansions. We are going to use some of their methods to calculate limiting forms for (76) for different frequency ranges of interest, but before that, we would like to establish some basic, general properties for $\sigma^2(t)$, $R_i(\tau)$ and $S_i(f)$.

Lemma 6.2

$$\lim_{t\to\infty}\frac{\sigma^2(t)}{t} = |V_0|^2\, S_N(0) \tag{77}$$

Corollary 6.2

$$\lim_{t\to\infty}\sigma^2(t) = \begin{cases} \infty & S_N(0)\neq 0 \\ \sigma^2(\infty) & S_N(0)=0\end{cases} \tag{78}$$

where $\sigma^2(\infty) < \infty$ is a finite nonnegative value.

For the models of burst and $1/f$ noise discussed in Section 5, we have

$$S_{Nburst}(0) = 1$$

from (61), and

$$S_{N1/f}(0) = \frac{4}{\gamma_c}$$

from (67). Thus $S_N(0) \neq 0$, and hence, $\lim_{t\to\infty} \sigma^2(t) = \infty$ are satisfied for both.

Since $\sigma^2(0) = 0$ we have

$$R_i(0) = 1 \tag{79}$$

and hence

$$\int_{-\infty}^{\infty} S_i(f)\mathrm{d}f = 1 \tag{80}$$

for any colored noise source. The total power $X_i X_i^*$ in the ith harmonic of the spectrum is preserved. The distribution of the power in frequency is given by $S_i(f)$. If

$$\lim_{t\to\infty} \sigma^2(t) = \infty \tag{81}$$

then $S_i(0)$ is nonnegative and *finite*, which is the case when the noise source spectrum extends to DC. On the other hand, when the noise source is bandpass, i.e., its spectrum does not extend to DC, then (81) will not be satisfied, and $S_i(f)$ will have a δ function component at $f = 0$. Now, we concentrate on the case when (81) is satisfied, i.e., when the spectrum takes a finite value at the carrier frequency (and its harmonics). Next, we proceed as Mullen and Middleton in [12, 13] and calculate limiting forms to the Fourier transform in (76) through approximating series:

Theorem 6.2 *Let (81) be true. For f away from 0, (76) can be approximated with*

$$S_i(f) \approx i^2 |V_0|^2 \frac{f_0^2}{f^2} S_N(f) \qquad f \gg 0 \tag{82}$$

where $\omega_0 = 2\pi f_0$. For f around 0, (76) can be approximated with

$$\begin{aligned} S_i(f) \approx \quad & \mathrm{F}\left\{\exp\left(-\frac{1}{2}\omega_0^2 i^2 |V_0|^2 S_N(0)|\tau|\right)\right\} + \\ & \mathrm{F}\left\{\exp\left(-\frac{1}{2}\omega_0^2 i^2 |V_0|^2 S_N(0)|\tau|\right)\right\} \circledast \\ & \mathrm{F}\left\{\omega_0^2 i^2 |V_0|^2 \left(|\tau|\int_{|\tau|}^{\infty} R_N(z)dz + \int_0^{|\tau|} z R_N(z)dz\right)\right\} \\ \approx \quad & \frac{f_0^2 i^2 \left(|V_0|^2 S_N(0)\right)}{\pi^2 f_0^4 i^4 \left(|V_0|^2 S_N(0)\right)^2 + f^2} + \frac{f_0^2 i^2 \left(|V_0|^2 S_N(0)\right)}{\pi^2 f_0^4 i^4 \left(|V_0|^2 S_N(0)\right)^2 + f^2} \circledast \\ & \mathrm{F}\left\{\omega_0^2 i^2 |V_0|^2 \left(|\tau|\int_{|\tau|}^{\infty} R_N(z)dz + \int_0^{|\tau|} z R_N(z)dz\right)\right\} \qquad f \approx 0 \end{aligned} \tag{83}$$

where $\circledast$ denotes convolution. The first term in (83) is a Lorentzian with corner frequency

$$\pi f_0^2 i^2 \left(|V_0|^2 S_N(0)\right)$$

and can be used as an approximation for (76) around $f = 0$ by ignoring the higher order second term. (83) contains the first two terms of a series expansion for (76).

From (82), we observe that the frequency dependence of $S_i(f)$ is as $1/f^2$ multiplied with the spectral density $S_N(f)$ of the noise source for offset frequencies away from the carrier. This result matches with measurement results for phase noise spectrum due to $1/f$ noise sources.

7 Phase noise and spectrum of an oscillator due to white and colored noise sources

In [1], we considered the case where the perturbation $b(t)$ is a vector of (uncorrelated) stationary, white Gaussian noise processes and obtained a stochastic characterization of the phase deviation $\alpha(t)$ and derived the resulting oscillator output spectrum, as we did it here for a colored noise source in Section 4 and Section 6. Now, we consider the case when both white and colored noise sources are present and unify our results. Let there be p white noise sources and M colored noise sources:

$$\frac{d}{dt}q(x) + g(x) + B_w(x)b_w(t) + \sum_{m=1}^{M} B_{cm}(x)b_{cm}(t) \tag{84}$$

where $B_w(.) : \mathbb{R}^n \to \mathbb{R}^{n\times p}$, $B_{cm}(\cdot) : \mathbb{R}^n \to \mathbb{R}^n$, $m = 1,\ldots,M$, $b_w(\cdot) : \mathbb{R} \to \mathbb{R}^p$ is a vector of (uncorrelated) stationary, white Gaussian noise processes, and $b_{cm}(\cdot) : \mathbb{R} \to \mathbb{R}$, $m = 1,\ldots,M$ are zero-mean, Gaussian, stationary colored stochastic processes (uncorrelated with each other, and with $b_w(t)$) with autocorrelation function/spectral density pairs

$$S_{Nm}(f) = \mathrm{F}\{R_{Nm}(\tau)\} \quad m = 1,\ldots,M$$

where

$$S_{Nm}(0) \neq 0 \quad m = 1,\ldots,M$$

and $R_{Nm}(\tau) \quad m = 1,\ldots,M$ are assumed to satisfy (54). In this case, the phase error $\alpha(t)$ satisfies the nonlinear differential equation

$$\begin{aligned} &\frac{\mathrm{d}\alpha(t)}{\mathrm{d}t} = v_1^T(t+\alpha(t)) \\ &\left[B_w(x_s(t+\alpha(t)))b_w(t) + \sum_{m=1}^{M} B_{cm}(x_s(t+\alpha(t)))b_{cm}(t)\right], \quad \alpha(0) = 0 \end{aligned} \tag{85}$$

where $v_1(t)$ is the periodically time-varying Floquet vector of Section 3. Let

$$c_w = \frac{1}{T}\int_0^T v_1^T(\tau)B_w(x_s(\tau))B_w^T(x_s(\tau))v_1(\tau)\mathrm{d}\tau \tag{86}$$

and

$$V_{0m} = \frac{1}{T}\int_0^T v_1^T(\tau)B_{cm}(x_s(\tau))\mathrm{d}\tau \quad m = 1,\ldots,M \tag{87}$$

Lemma 7.1 *$\alpha(t)$ that satisfies (85) becomes a Gaussian random variable with constant mean, and variance given by*

$$\begin{aligned} \sigma^2(t) &= c_w t + \sum_{m=1}^{M} 2|V_{0m}|^2 \int_0^t (t-\tau)R_{Nm}(\tau)d\tau \\ &= c_w t + \sum_{m=1}^{M} 2|V_{0m}|^2 \int_{-\infty}^{\infty} S_{Nm}(f)\frac{(1-\exp(j2\pi f t))}{4\pi^2 f^2}df \end{aligned}$$

for t large enough such that

$$\exp\left(-\frac{1}{2}\omega_0^2(i-k)^2\sigma^2(t)\right) \approx \begin{cases} 1 & i = k \\ 0 & i \neq k \end{cases} \tag{88}$$

Theorem 7.1 *With $\alpha(t)$ characterized as above, the oscillator output $x_s(t+\alpha(t))$ is a stationary process, and its spectral density is given by*

$$S_V(f) = \sum_{i=-\infty}^{\infty} X_i X_i^* \, S_i(f + i f_0) \tag{89}$$

where X_i are the Fourier series coefficients of $x_s(t)$, and

$$S_i(f) = \begin{cases} \frac{f_0^2 i^2 \left(c_w + \sum_{m=1}^{M} |V_{0m}|^2 S_{Nm}(0)\right)}{\pi^2 f_0^4 i^4 \left(c_w + \sum_{m=1}^{M} |V_{0m}|^2 S_{Nm}(0)\right)^2 + f^2} & f \approx 0 \\ i^2 \frac{f_0^2}{f^2}\left(c_w + \sum_{m=1}^{M} |V_{0m}|^2 S_{Nm}(f)\right) & f \gg 0 \end{cases} \tag{90}$$

The full spectrum of the oscillator with white and colored noise sources has the shape of a Lorentzian around the carrier, and away from the carrier, the white noise sources contribute a term that has a $1/f^2$ frequency dependence, and the colored noise sources contribute terms that have a frequency dependence as $1/f^2$ multiplied with the spectral density of the colored noise source.

8 Examples

We have derived an *analytical* expression, given by (89) and (90), for the spectrum of the oscillator output with phase noise due to white and colored noise sources. The analytical expression in (89) and (90) contains some parameters to be computed:

- X_i: The Fourier series coefficients of the large-signal *noiseless* periodic waveform $x_s(t)$ of the oscillator output.
- $c_w = \frac{1}{T}\int_0^T v_1^T(\tau)B_w(x_s(\tau))B_w^T(x_s(\tau))v_1(\tau)\mathrm{d}\tau$: Scalar that characterizes the contributions of the white noise sources.
- $V_{0m} = \frac{1}{T}\int_0^T v_1^T(\tau)B_{cm}(x_s(\tau))\mathrm{d}\tau \;\; m = 1,\ldots,M$: Scalars that characterize the contributions of the colored noise sources.

Once the periodic steady-state $x_s(t)$ of the oscillator and the scalars c_w and $V_{0m},\ m = 1,\ldots,M$ are computed, we have an analytical expression that gives us the spectrum of the oscillator at *any* frequency f. The computation of the spectrum is *not* performed separately for every frequency of interest. We compute the whole spectrum as a function of frequency *at once*, which makes our technique very efficient. Using the results of the theory developed in this work, an analysis and design tool for low phase noise oscillator design was implemented in an in-house circuit simulator.

Oscillator with parallel RLC and a nonlinear current source

We now present simulation results in the phase noise characterization of a simple oscillator in Figure 1(a). The resistor is assumed to be noiseless, but we insert a stationary external current noise source across the capacitor. The Floquet vector $v_1(t)$ is a two-dimensional vector, since the oscillator has two state variables, namely the capacitor voltage and the inductor current. Figure 1(b) shows the entry of $v_1(t)$ corresponding to the capacitor voltage.

Now, let us assume that we have two current noise sources across the capacitor, one of them a white stationary noise source, and the other a colored stationary noise source with bandwidth much smaller than the oscillation frequency. To calculate the spectrum of the capacitor voltage given by (89) and (90), we need to compute c_w in (86) for the white noise source, and V_0 in (87) for the colored noise source. For stationary noise sources, $B_w(t)$ in (86) and $B_c(t)$ in (87) are constant functions of time t. Figure 1(c) shows $v_1^T(t)B_wB_w^Tv_1(t)$ which is a periodic function of time t. Note that c_w is the time-average of this quantity.

From (87), we observe that V_0 is the time-average of $v_1^T(t)B_c$. The time-average of $v_1(t)$ in Figure 1(b) for the capacitor voltage is 0! Thus, we conclude that any *stationary* (with the modulation $B_c(t)$ a constant function of time) colored noise source (with bandwidth much smaller than the oscillation frequency) connected across the capacitor has no contribution to the oscillator spectrum due to phase noise, because $V_0 = 0$ for this noise source.

CMOS ring-oscillator

A ring-oscillator with CMOS inverter delay cells was simulated for its phase noise spectrum. It oscillates at 2.86 GHz and burns 150 mW. Figure 2 shows $S_1(f)$ in (90) using the expression for $f \gg 0$. Contributions of the thermal (white) and $1/f$ (colored) noise sources, as well as the total spectrum, are plotted.

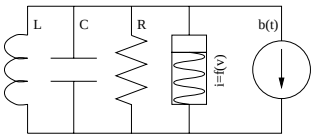

(a) Simple oscillator

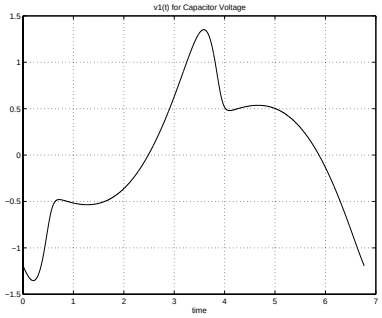

(b) $v_1(t)$ for the capacitor voltage

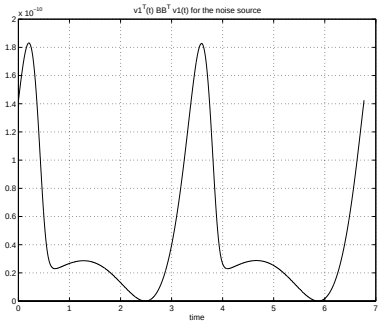

(c) $v_1^T(t)B_wB_w^Tv_1(t)$ for the noise source

Figure 1: Simple oscillator with parallel RLC-nonlinearity

Acknowledgments

We would like to thank Jaijeet Roychowdhury, Hans Georg Brachtendorf, David Lee, Amit Mehrotra, Peter Feldmann and Bob Melville for useful discussions.

References

[1] A. Demir, A. Mehrotra, and J. Roychowdhury. Phase noise in oscillators: A unifying theory and numerical methods for characterisation. In *ACM/IEEE Design Automation Conference*, June 1998.

[2] R. März. On linear differential-algebraic equations and linearizations. *Applied Numerical Mathematics*, 18, September 1995.

[3] R. Lamour, R. März, and R. Winkler. How floquet theory applies to differential-algebraic equations. preprint, 1997.

[4] M. Farkas. *Periodic Motions*. Springer-Verlag, 1994.

[5] P.A. Selting and Q. Zheng. Numerical stability analysis of oscillating integrated circuits. *Journal of Computational and Applied Mathematics*, 82(1,2):367–378, September 1997.

[6] R. Telichevesky, K.S. Kundert, and J. White. Efficient steady-state analysis based on matrix-free krylov-subspace methods. In *Proc. Design Automation Conference*, June 1995.

[7] C.W. Gardiner. *Handbook of Stochastic Methods for Physics, Chemistry and the Natural Sciences*. Springer-Verlag, 1983.

[8] H. Risken. *The Fokker-Planck Equation*. Springer-Verlag, 1989.

[9] P.R. Gray and R.G. Meyer. *Analysis and Design of Analog Integrated Circuits*. John Wiley & Sons, second edition, 1984.

[10] M.S. Keshner. $1/f$ noise. *Proceedings of the IEEE*, 70(3):212, March 1982.

[11] F. X. Kaertner. Analysis of white and $f^{-\alpha}$ noise in oscillators. *International Journal of Circuit Theory and Applications*, 18:485–519, 1990.

[12] J.A. Mullen and D. Middleton. Limiting forms of fm noise spectra. *Proceedings of the IRE*, 45(6):874–877, June 1957.

[13] D. Middleton. *An Introduction to Statistical Communication Theory*. IEEE Press, 1996.

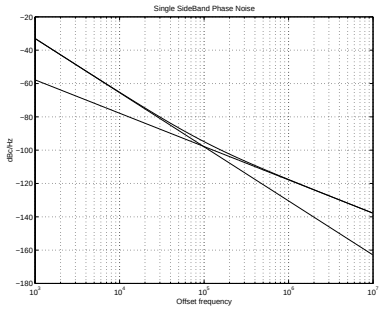

Figure 2: CMOS ring-oscillator